Mechanism Involved in Generating the Carboxyl-Terminal Half Topology of P-Glycoprotein†

Ernest S. Han and Jian-Ting Zhang*,‡

Department of Physiology and Biophysics, University of Texas Medical Branch, Galveston, Texas 77555-0641

Received March 26, 1998; Revised Manuscript Received June 18, 1998

ABSTRACT: P-Glycoprotein (Pgp) is a polytopic membrane protein that consists of a tandem repeat of a transmembrane (TM) domain followed by a nucleotide-binding domain. For the carboxyl-terminal half (C-half) of Pgp, at least three different topological orientations have been observed. One major difference between these topologies is reflected in the membrane insertion property of TM8, which is predicted to (1) function as a stop-transfer sequence, (2) lack stop-transfer activity, or (3) function as a signal-anchor sequence. To understand the mechanism involved in generating multiple topological forms for the C-half of Pgp, we investigated the membrane insertion properties of TM segments using the Chinese hamster *pgp1* Pgp as a model protein in a cell-free system. We found that TM8 alone or in the presence of TM7 functions as a signal-anchor sequence to insert into membranes with a cytoplasmic amino terminus and an extra-cytoplasmic carboxyl terminus. However, TM8 displayed stop-transfer activity when linked to the C-terminal end of the signal-anchor sequence, TM1. In addition, the membrane orientation of TM8 was found to be regulated by the charge distribution flanking TM8. Interestingly, we found that mammalian and wheat germ ribosomes differentially regulate the signal-anchor and stop-transfer properties of TM8. We conclude that the unique topogenic properties of TM8 direct the generation of multiple C-half topological orientations.

Generation of transmembrane (TM)[1] topology for integral membrane proteins has been extensively studied over the past decade (for reviews, see *1*−*3*). Numerous studies have focused on the mechanisms involved in determining the orientation of a single TM segment. However, the topogenesis of proteins containing multiple TM segments (polytopic proteins) is not well understood. It is postulated that the first TM segment functions as a signal-anchor sequence and the second TM segment functions as a stop-transfer sequence (*4*, *5*). This signal-anchor and stop-transfer event repeats for downstream TM segments until every TM segment inserts into the membrane. Analysis of the most N-terminal signal-anchor sequence revealed a bias in the net charge distribution of the flanking 15 amino acids which generally predicted its TM orientation and consequently specified the topology of downstream TM segments (*5*). Sipos and von Heijne (*6*) later proposed that this net charge bias applied to all TM segments in a polytopic membrane protein, but was less influential for more C-terminal segments. Furthermore, the effect of charged residues on membrane topology may differ depending on whether prokaryotic or eukaryotic cells are used (*7*). Although the distribution of charged amino acids is important for determining the orientation of a TM segment, other mechanisms such as folding of the N-terminal region, the hydrophobicity of a TM segment, and anionic phospholipids may also be involved (*8*−*10*).

The topology of the polytopic membrane protein, P-glycoprotein (Pgp), has been extensively studied. Pgp is thought to consist of two homologous halves, each containing six putative TM segments followed by a nucleotide-binding domain (*11*). However, several studies suggest that the insertion of Pgp TM segments may be more complex than originally thought. For the carboxyl-terminal half (C-half) of Pgp, two studies have confirmed the existence of a hydropathy-predicted topology (*12*, *13*). But other topological forms of the C-half have also been observed (*14*−*18*). According to the sequential membrane insertion theory, TM7 in the C-half of Pgp is predicted to function as a signal-anchor sequence that inserts into membranes with a cytoplasmic N-terminus and an extra-cytoplasmic C-terminus (N_{cyt}-C_{exo}), while TM8 functions as a stop-transfer sequence. However, in one alternative folding of Pgp, TM8 was suggested to translocate into the ER lumen and thus did not stop the membrane translocation event (*14*, *15*, *17*, *18*). In another model, TM8 was thought to function as a signal-anchor sequence which inserts into membranes in a N_{cyt}-C_{exo} orientation while TM7 consists of two TM segments, one of which functions presumably as a signal-anchor sequence and the other as a stop-transfer sequence (*16*).

† This work was supported by grants from the National Institutes of Health (CA 64539, GM55398) and U. S. Army Medical Research and Materiel Command (DAMD17-94-J-4419). E.S.H. is a recipient of a predoctoral fellowship from the U. S. Army Medical Research and Materiel Command (DAMD17-94-J-4080). J.-T.Z. is a recipient of a Career Investigator Award from the American Lung Association.

* To whom correspondence should be addressed. Telephone: (317) 278-4503. Fax (317) 274-7714.

‡ Current address: Department of Pharmacology and Toxicology, Cancer Center, Building R4, Room 166, Indiana University School of Medicine, 1044 W. Walnut St., Indianapolis, IN 46202.

[1] Abbreviations: TM, transmembrane; Pgp, P-glycoprotein; RRL, rabbit reticulocyte lysate; WGE, wheat germ extract; PNGase F, peptide *N*-glycosidase F; endo H, endoglycosidase H; RM, rough microsomes; C-half, carboxyl-terminal half; N-half, amino-terminal half.

S0006-2960(98)00702-8 CCC: $15.00
Published on Web 08/05/1998

To understand the mechanism by which the C-half topology of Pgp is generated, we examined the membrane insertion properties of TM segments from the C-half of Chinese hamster *pgp1* Pgp. We demonstrated that the predicted cytoplasmic loop linking putative TM8 and TM9 is extra-cytoplasmic. Exposure of this loop to the extracytoplasmic space was in part determined by the unique membrane insertion properties of putative TM8, which was found to have both signal-anchor and stop-transfer activities. Both the net charge distribution flanking TM8 and ribosomes were also found to modify the membrane insertion and topological orientation of TM8. These results suggest that the topogenic properties of TM8 may be important in the generation of C-half Pgp topologies.

EXPERIMENTAL PROCEDURES

Pgp Constructs. A *Sac*I−*Xba*I fragment encoding the six putative transmembrane segments of the C-terminal half Chinese hamster *pgp1* Pgp (Met^{613} to Leu^{1093}) was subcloned into the *Sac*I and *Xba*I sites of the pGEM-4z expression vector (Promega) to create the plasmid pGHaPGP-C6.

To generate the chimeric Pgp molecule, TM1/8R, we performed recombination PCR (*19*). Briefly, a cassette containing TM8 was amplified by PCR using pGHaPGP-C6 template and chimeric primers (5′-GAATTCAACCATGTAT-3′ and 5′-GCTTCAGACATCTTTAATACT-3′). A second PCR reaction was performed using the amplified cassette, the universal SP6 primer, and pGPGP-N3 template (*20*), and the PCR product was ligated into a pGEM T-easy vector (Promega) (pTez-TM1/8R). Plasmid pTez-TM1/8R was digested with *Eco*RI followed by T4 polymerase treatment and then further digested with *Kpn*I to create a fragment containing TM1 and TM8. This fragment, together with a *Ssp*I−*Hin*dIII fragment from the plasmid pGPGP-N3, which contains a glycosylation reporter (*20*), was ligated to a fresh pGEM-4z vector digested with *Kpn*I and *Hin*dIII. The resulting TM1/8R plasmid encodes TM1 with its flanking sequences (Met^{1}−Phe^{101}) followed by TM8 and its flanking sequences (Asn^{739}−Met^{788}) and a reporter molecule. Plasmid TM8R, which encodes TM8 with its flanking sequences (Asn^{739}−Met^{788}) followed by a reporter, was also created by the recombination PCR method as described above. TM1/8R template, SP6 primer, and a hybrid primer (5′-TTCATCATCAGTATTCTCCATCACG-3′) were used for the first PCR. TM1/8R template, universal primer T7, and the product from the first PCR were used for the second PCR. The final PCR product was ligated into the *Hin*cII site of pGEM-4z vector.

Plasmid TM7-8R was created by ligating three fragments together: *Gsu*I−*Hin*dIII fragment (encodes the reporter) from plasmid TM1/8R, a *Sac*I−*Gsu*I fragment (encodes Met^{613}−Met^{788}, which includes TM7 and TM8) from plasmid pGHaPGP-C6, and a fresh pGEM-4z vector digested with *Sac*I and *Hin*dIII. TM7-8(RRR)R was similarly created except a *Sac*I−*Gsu*I fragment was obtained from the plasmid RRR (see below). To generate the plasmid TM1R, pGPGP-N3 DNA (*20*) was digested with *Bgl*II, and a blunt end was created by treatment with Klenow fragment. The DNA was further digested with *Bsa*AI to remove TM2 and TM3 encoding sequences and then self-ligated. TM1R encodes Met^{1}−Phe^{101} followed by the reporter molecule.

For plasmids TM1-2R and TM7R, a one-step PCR reaction was performed using the following template and primers: for TM1-2R, pGPGP-N3 template, primers B660 (5′-GCCTCGAGTTTTGTCACCAATTCC-3′) and SP6; for TM7R, pGHaPGP-C6 template (TM7R), primers A693a (5′-GTCGTGATGGAGTCCTTTTGGCGT-3′) and B746a (5′-CAAGATCTGTCGTTTGGTTTC-3′). For TM1-2R, the PCR product was digested with *Xho*I and *Hin*dIII and ligated into the plasmid pGPGP-N3 digested with the same two enzymes. Plasmid TM1-2R encodes the amino acids Met^{1}−Lys^{186} followed by a reporter molecule. For TM7R, the amplified product was digested with *Bgl*II and ligated to a pGEM-4z vector along with the reporter sequence (plasmid pGPGP-N3 digested with *Bgl*II and *Hin*dIII). Plasmid TM7R encodes the amino acids Ser^{693}−Arg^{746} followed by a reporter molecule. The N-terminal end of TM7R contains two additional amino acids (Met and Glu), generated from the engineered translation initiation codon in the cDNA construct.

Mutations involving the addition of charged amino acids into the Pgp sequence were generated either by Kunkel mutagenesis (for E779R and RRR mutants; see ref *21*) or by site-directed mutagenesis using two PCR steps (for E779D, E779Q, K776E; ref *21*). Oligonucleotides used to generate the mutations were as follows: (E779R) 5′-AGCTGGACGGATCCTCA-3′; (RRR) 5′-TTTGGCAAACGTCGACGAGCTGGAGAG-3′; (E779Q) 5′-GGCAAAGCCGGCCAGATCCTC-3′; (E779D) 5′-GGCAAAGCCGGCGATATCCTC-3′; (K776E) 5′-TTGGCGAAGCCGGCGAGATC-3′. For all DNA constructs, DNA sequencing was performed to confirm the fidelity of the sequence and presence of introduced mutations and to ensure proper linkages during subcloning procedures.

In Vitro Transcription and Translation Using a Cell-Free System. In vitro transcripts were created as described by Zhang and Ling (*14*). The following restriction enzymes were used to create runoff transcripts: *Hin*dIII (TM1/8R, TM8R, TM1R, TM1-2R), *Hae*II (TM7R), and *Xba*I (pGHaPGP-C6, all charge mutant constructs). Translation of the runoff transcripts was performed using the rabbit reticulocyte lysate translation system as suggested by the supplier (Promega) in the absence or presence of dog pancreatic microsomal membranes [isolated as described by Walter and Blobel (*22*) and also obtained from Promega and Boehringer Mannheim]. Membrane (pellet) and soluble (supernatant) fractions were separated by centrifugation at maximum speed (≈13 000−14 000 rpm) using a tabletop microcentrifuge at 4 °C for 15 min (all centrifugations were performed using this speed and temperature unless otherwise noted). Alkaline extraction of membrane-associated proteins was performed by incubating translation products in 10 mM Na_2CO_3, pH 11.7, on ice for 30 min. The suspension was centrifuged for 15 min to separate membrane and soluble fractions.

Membrane Topology Determination. The pellet fraction was resuspended in STBS solution (in mM: 250 sucrose, 10 Tris-HCl, pH 7.5, 150 NaCl) and incubated with or without proteinase K (0.2 mg/mL final concentration) for 20 min at room temperature. After stopping the reaction by addition of phenylmethylsulfonyl fluoride (PMSF) (10 mM final concentration), the sample was centrifuged for 10 min and washed once in STBS containing PMSF.

For experiments requiring endoglycosidase PNGase F treatment, samples were centrifuged for 10 min, and the

membrane pellet was resuspended in a buffer containing 50 mM sodium phosphate buffer (pH 7.6), 1.25% Nonidet P-40 (or Triton X-100 for immunoprecipitation experiments), 0.5% 2-mercaptoethanol, 2 mM PMSF, 0.2% SDS, and 1 unit of PNGase F or an equivalent volume of water in a control reaction. The reaction was incubated for 1 h at 37 °C and stopped by addition of electrophoresis sample buffer. Endoglycosidase H treatment was performed as suggested by the manufacturer (New England Biolabs).

Immunoprecipitation was carried out using samples obtained after endoglycosidase treatment. Samples were incubated with anti-Pgp polyclonal antibody α-Pgp-L8 (*18*) overnight at 4 °C and then incubated with 3% bovine serum albumin-absorbed Protein A beads (final concentration ≈25 mg/mL) for at least 2 h on a shaker at room temperature. Following centrifugation at room temperature, the pellet was washed twice in a buffer containing 0.1% Triton X-100, 0.02% SDS, 150 mM NaCl, 50 mM Tris-HCl, pH 7.4, 5 mM EDTA, and 10 mM PMSF.

For the analysis of C-half topogenesis in the presence of wheat-germ ribosomes, we isolated wheat-germ ribosomes from crude wheat-germ extracts by centrifugation as described by Wang et al. (*23*). Approximately 6 μg of ribosomes was added to the rabbit reticulocyte lysate translation mix to a final concentration of 10% (v/v). RNA transcripts were then added to initiate the translation reaction. After translation, membrane-associated translation products were isolated as described above. All samples were analyzed by SDS−polyacrylamide gel electrophoresis (SDS−PAGE) and fluorography. For quantification of bands, densitometric scanning of fluorographs was performed using Quantity One (v.2.4) software.

RESULTS

Membrane Topology of the C-Terminal Half of Chinese Hamster pgp1 Pgp. We used the Chinese hamster *pgp1* Pgp as a model protein to determine the mechanism involved in generating C-half Pgp topology. Using the rabbit reticulocyte lysate (RRL) system, translation of a RNA transcript encoding the C-half TM domain of Chinese hamster *pgp1* Pgp (pGHaPGP-C6) resulted in a 48-kDa product (Figure 1B, lane 1). In the presence of dog pancreatic microsomal membranes (RM), an additional 51-kDa protein was produced (Figure 1B, lane 2). To separate integrally associated proteins from peripheral and lumen content proteins, we treated membranes with Na_2CO_3, pH 11.7 (see Experimental Procedures and ref *24*). As shown in Figure 1B, a majority of the 51- and 48-kDa products remained in the pellet fraction (lanes 3−6). However, all of the 48-kDa protein translated in the absence of RM were found in the supernatant fraction after sodium carbonate treatment (data not shown). Thus, the majority of 51- and 48-kDa proteins translated in the presence of RM inserted into membranes. Treatment with endoglycosidase PNGase F reduced the 51-kDa band to 48 kDa, suggesting that the 51-kDa protein was glycosylated with a high-mannose core (assuming a calculated size of ~2.5 kDa) (Figure 1B, lanes 7, 8).

There are two N-linked glycosylation consensus sites in the C-half of Chinese hamster *pgp1* Pgp that are not utilized based on hydropathy analysis (Figure 1A). One is at the N-terminal end before putative TM7, and another is located

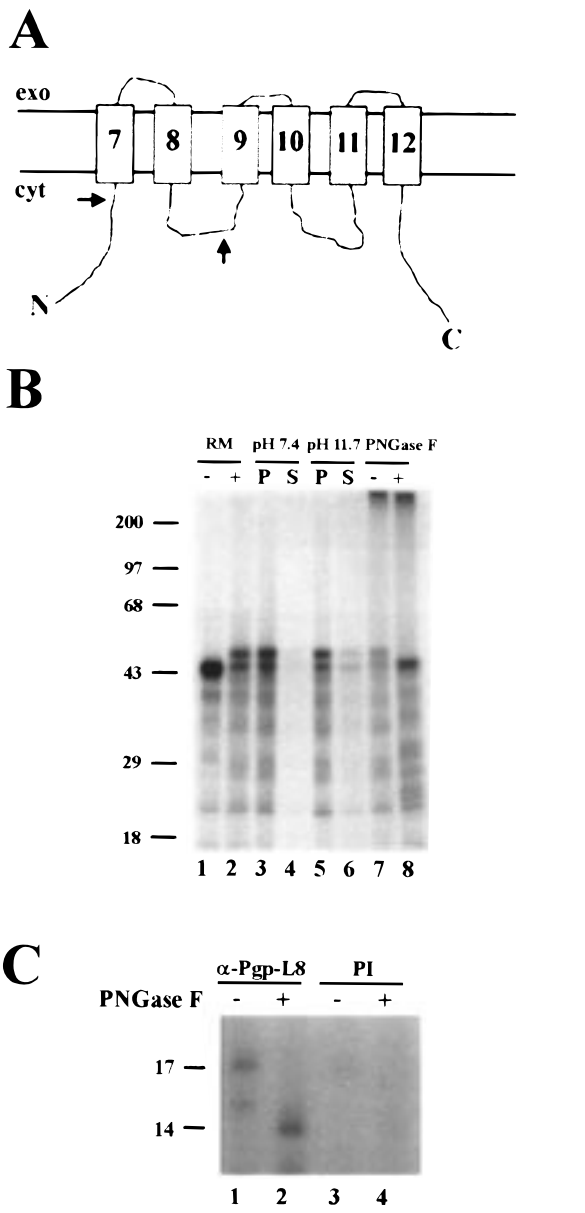

FIGURE 1: Membrane topology of C-terminal P-glycoprotein. (A) Schematic diagram of C-terminal P-glycoprotein based on hydropathy analysis. Arrows denote the approximate location of the consensus sequence for N-linked glycosylation. The symbols exo, cyt, N, and C denote extra-cytoplasmic space, cytoplasmic space, N-terminus, and C-terminus, respectively. (B) Translation of the C-half TM domain (pGHaPGP-C6) in a cell-free system. Translation was performed using RRL in the absence (lane 1) or presence (lane 2) of RM. After translation, the protein products were either separated into membrane (pellet, P) and nonmembrane (supernatant, S) fractions by centrifugation (lanes 3, 4) or treated first with Na_2CO_3, pH 11.7, followed by centrifugation (lanes 5, 6). Glycosylation of protein products was determined by treating membrane-associated fractions with PNGase F (lanes 7, 8). (C) Location of N-linked glycosylation in C-half Pgp. A polyclonal antibody (α-Pgp-L8, ref *18*), raised against a peptide corresponding to the loop linking putative TM8 and TM9, was used for immunoprecipitation of peptides remaining after exposure of RM to proteinase K (0.2 mg/mL) (lane 1) or proteinase K and PNGase F (lane 2). Similar studies were conducted with preimmune serum (lanes 3 and 4).

in the loop linking putative TM8 and TM9. To determine which glycosylation site was used, we treated RM containing pGHaPGP-C6 translation products with proteinase K followed by immunoprecipitation with a polyclonal antibody raised against the loop linking TM8 and TM9 (α-Pgp-L8;

ref *18*). A 17-kDa protease-resistant peptide that shifted to 14 kDa after PNGase F treatment was immunoprecipitated with α-Pgp-L8 (Figure 1C, lanes 1, 2), but not with preimmune serum (Figure 1C, lanes 3 and 4). This peptide was also not observed if RM was digested in the presence of 1% Triton X-100 (data not shown). These results indicate that the glycosylation occurs at the consensus site located in the loop between TM8 and TM9 and thus suggest a topology different than predicted by hydropathy analysis. The glycosylated 17-kDa product was also observed after proteinase K treatment of membrane-associated full-length Pgp molecules, suggesting that the unexpected topology of the C-half Pgp did not result from the absence of N-half Pgp (data not shown).

Effect of Positively Charged Amino Acids following Putative TM8 on Generation of C-Half Pgp Topology. Based on a model from Béjà and Bibi (*16*) for C-half Pgp topology, TM8 is predicted to function as a signal-anchor sequence that initiates membrane insertion in a N_{cyt}-C_{exo} orientation (see Figure 2A). Since the charged residues that flank TM segments largely determine the orientation of a signal-anchor sequence (*5*), adding positive charges C-terminal to TM8 may alter the N_{cyt}-C_{exo} signal-anchor property of TM8. To test this hypothesis, we modified the charge distribution immediately following TM8 by replacing glutamic acid residue 779 with arginine (E779R), glutamine (E779Q), or aspartic acid (E779D) in pGHaPGP-C6 (Figure 2B). After translation in RRL, membrane-integrated products were isolated following sodium carbonate treatment, and the effects of mutations on the generation of the glycosylated 51-kDa product, which corresponds to the alternative topology, were monitored. As shown in Figure 2C,D, the glycosylated 51-kDa band from E779R products decreased by 24% compared to wild-type, while a decrease of only 9% was observed for E779Q. There was virtually no change in the 51-kDa band for E779D. The reduction in the 51-kDa band was not specific for glutamic acid residue 779 because an even greater reduction (43%) in the 51-kDa band was observed if three arginines (RRR) were added after lysine residue 776 (Figure 2C, lane 5). In addition, when we decreased the net positive charge after TM8 by replacing lysine residue 776 with glutamic acid, a 39% increase in the 51-kDa band compared to wild-type was observed (Figure 2C, lane 6). If these mutations affect the glycosylation of the reporter, we would expect an unglycosylated reporter that is resistant to proteinase K digestion. However, proteinase K digestion failed to generate unglycosylated, membrane-protected peptide fragments (data not shown). Therefore, the effect of the mutations of charged amino acids on C-half topology was not due to alterations in glycosylation efficiency. Taken together, our results suggest that the TM8 from the C-half of Pgp may have signal-anchor activity for N_{cyt}-C_{exo} insertion, and this activity of TM8 can be regulated by the charged residues flanking TM8.

Signal-Anchor Activity of TM8 in the Topogenesis of C-Half Pgp. To examine more directly the signal-anchor activity and membrane orientation of TM8, we created a truncated Pgp construct containing a glycosylation reporter linked to the C-terminal end of TM8 (TM8R; Figure 3A). To retain the integrity of the membrane insertion property of TM8, its flanking N- and C-terminal 15 amino acids were included in the construct since the 15 amino acids flanking

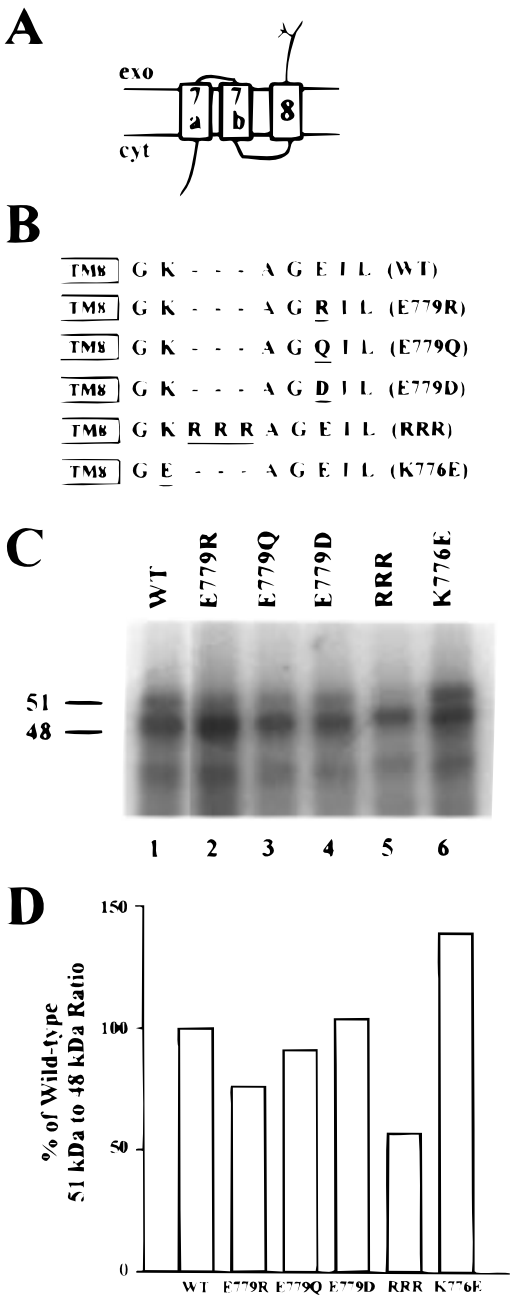

FIGURE 2: Effect of charged amino acids immediately C-terminal to TM8 on generation of Pgp C-half topologies. (A) Topological model of C-half Pgp proposed by Béjà and Bibi (*16*). The branched symbol represents N-linked glycosylation. Other symbols were described in Figure 1A. (B) Schematic diagram of the partial amino acid sequence for wild-type and mutant Pgp constructs. Differences in the amino acid sequence from wild-type Pgp are underlined in the mutant amino acid sequences. (C) Translation of mutant pGHaPGP-C6. RNA transcripts encoding wild-type C-terminal half Pgp (pGHaPGP-C6, lane 1) or Pgp containing mutations which altered the charge C-terminal to TM8 (lanes 2−6) were translated using the RRL system. Membrane-integrated Pgp molecules were isolated after Na_2CO_3 treatment and analyzed by SDS−PAGE and fluorography. (D) Quantification of the topology of Pgp C-half constructs. The membrane-integrated 51-kDa and 48-kDa products were quantified by densitometric scanning of fluorographs. For each experiment, the ratio of 51-kDa band to 48-kDa band was determined for each Pgp construct, and the ratios for all mutant Pgp constructs were then normalized to the ratio of the wild-type Pgp construct. Values represent the average of four experiments.

a TM segment are thought to be important in determining TM orientation (*5*). Translation of TM8R in RRL resulted

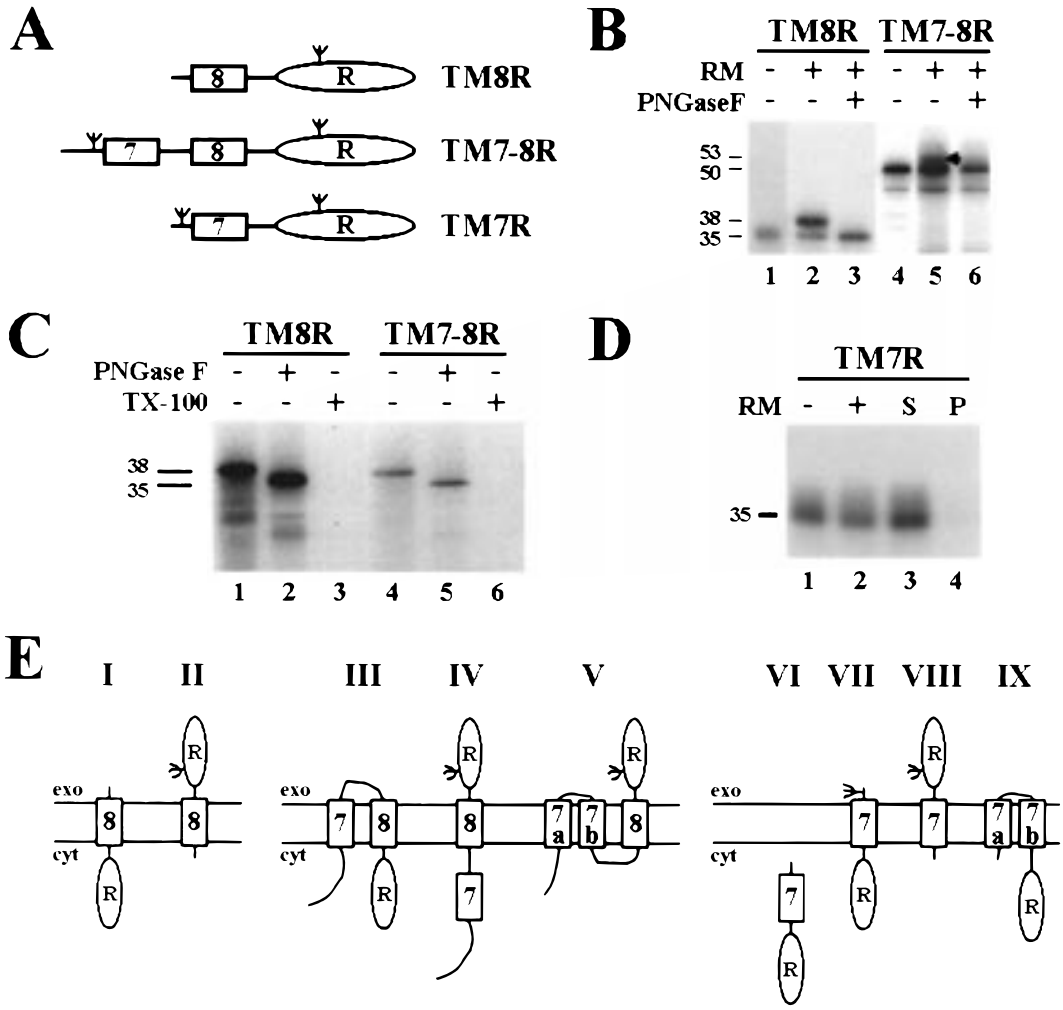

FIGURE 3: Membrane insertion and topology of TM7 and TM8. (A) Schematic diagram of the Pgp constructs, TM8R, TM7-8R, and TM7R. Putative TM segments are shown as rectangular boxes, and the glycosylation reporter molecule is indicated as an oval. Branched symbols denote consensus sites for N-linked glycosylation. (B) Analysis of N-linked glycosylation for TM8R and TM7-8R. Lanes 1 and 4 represent translation products in the absence of RM. Lanes 2 and 5 and lanes 3 and 6 show membrane-associated products without or with PNGase F treatment, respectively. (C) Proteinase K treatment of RM containing TM8R or TM7-8R translation products. Proteinase K digestion was performed in the absence (lanes 1 and 4) or presence of Triton X-100 (lanes 3 and 6). Membrane-protected fragments were further treated with PNGase F (lanes 2 and 5). (D) Membrane insertion of putative TM7. Translation of TM7R in RRL was performed in the absence (lane 1) or presence (lane 2) of RM. Supernate and pellet fractions were separated after centrifugation (lanes 3, 4). (E) Topological models for TM8R (models I and II), TM7-8R (models III−V), and TM7R (models VI−IX). See panel A for description of symbols.

in a 35-kDa product (Figure 3B, lane 1). In the presence of RM, a majority of TM8R products shifted to 38 kDa and were membrane-associated (Figure 3B, lane 2). This 38-kDa band was sensitive to PNGase F treatment (Figure 3B, lane 3) and resistant to proteinase K digestion (Figure 3C, lanes 1, 2). These results suggest that the large reporter domain (≈32 kDa) of TM8R was translocated into the RM lumen and glycosylated (see Figure 3E, model II). Thus, TM8 alone contains a signal-anchor activity and inserts into membranes predominantly in a N_{cyt}-C_{exo} orientation.

To test if TM8 maintains the signal-anchor activity in the presence of TM7, we constructed a fusion Pgp molecule containing TM7 and TM8 followed by a glycosylation reporter (TM7-8R; Figure 3A). We reasoned that if TM8 in the TM7-8R construct maintains the signal-anchor activity to initiate N_{cyt}-C_{exo} insertion, then the reporter of TM7-8R will be translocated into the RM lumen and glycosylated (see models IV and V, Figure 3E). Translation of TM7-8R in the absence of RM resulted in a 50-kDa product (Figure 3B, lane 4). In the presence of RM, a 53-kDa membrane-associated product was also observed (Figure 3B, lane 5; arrow). The 53-kDa product shifted to 50 kDa after PNGase F treatment, indicating the presence of N-linked glycosylation (Figure 3B, lanes 5, 6). To determine if the reporter of the glycosylated TM7-8R is in the RM lumen, we performed proteinase K digestion of membrane-associated TM7-8R products. We observed a membrane-protected 38-kDa band that shifted to 35 kDa after PNGase F treatment (Figure 3C, lanes 4, 5). The size of this glycosylated membrane-protected band is the same as the membrane-protected reporter of TM8R. Thus, the reporter of the glycosylated TM7-8R is located in the RM lumen and glycosylated. These results suggest that TM8 can initiate insertion into membranes in a N_{cyt}-C_{exo} orientation in the presence of putative TM7 (Figure 3E, models IV and V). The strong de novo signal-anchor activity of TM8 which initiates N_{cyt}-C_{exo} insertion is consistent with the alternative topology proposed by Béjà and Bibi (*16*).

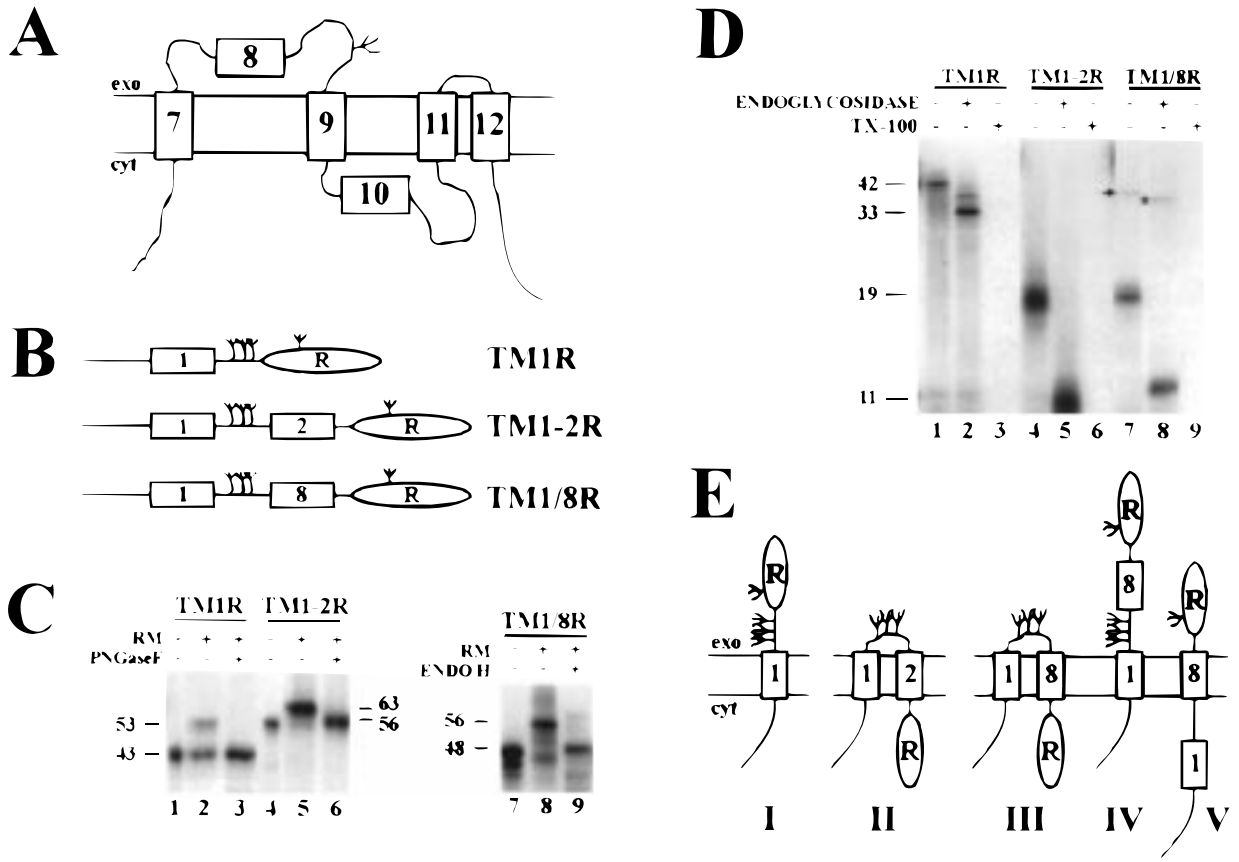

FIGURE 4: Stop-transfer activity of putative TM8. (A) Topological model of C-half Pgp based on a previous study by Zhang et al. (*14*). See Figure 1A for symbols. (B) Schematic diagram of the Pgp constructs, TM1R, TM1-2R, and TM1/8R. See Figure 3A for description of symbols. (C) Analysis of N-linked glycosylation for TM1R, TM1-2R, and TM1/8R. Lanes 1, 4, and 7 represent translation products in the absence of RM. Lanes 2 and 5 and lanes 3 and 6 show membrane-associated products without or with PNGase F treatment, respectively. Lanes 8 and 9 show membrane-associated products without or with endoglycosidase H treatment, respectively. (D) Proteinase K treatment of RM containing TM1R, TM1-2R, or TM1/8R translation products. Proteinase K digestion was performed in the absence (lanes 1, 4, and 7) or presence of Triton X-100 (lanes 3, 6, and 9). Membrane-protected fragments were further treated with PNGase F (lanes 2 and 5) or endo H (lane 8). We noted a minor 38-kDa product for TM1/8R (lane 8, see arrow) that shifted to 35 kDa after endo H treatment (lane 9, see asterisk). (E) Topological models for TM1R (model I), TM1-2R (model II), and TM1/8R (models III−V).

Since our results suggest that TM8 in the presence of TM7 can function as a signal-anchor sequence, TM7 may fold into membranes as two TM segments as proposed by Béjà and Bibi (*16*; see Figure 3E, model V). Therefore, we examined the membrane insertion properties of TM7 by creating a construct containing TM7 followed by a glycosylation reporter (TM7R; Figure 3A). Translation in the absence or presence of RM both resulted in a 35-kDa product (Figure 3D, lanes 1, 2), suggesting that no glycosylation occurred in the presence of RM. When we tested the membrane integration properties of TM7R product, we found that the 35-kDa product was not associated with the membrane fraction after centrifugation (Figure 3D, lanes 3, 4). These results suggest that TM7 alone cannot insert into membranes (Figure 3E, model VI). Therefore, TM7 likely does not have de novo membrane insertion activities (see Discussion).

Stop-Transfer Activity of TM8 in the Topogenesis of C-Half Pgp. The above results suggest that TM8 has a strong signal-anchor activity to initiate the N_{cyt}-C_{exo} orientation and supports the alternate topology proposed by Béjà and Bibi (*16*). In previous studies (*14*, *15*, *17*, *18*), other alternative topologies were also proposed where TM8 was translocated to the extracellular space, likely due to the lack of stop-transfer activity (see one example in Figure 4A). To test the stop-transfer activity of TM8, we engineered a TM1/8R construct by replacing TM2 of Pgp (Figure 4B). To establish that TM1 is a signal-anchor sequence and TM2 is a stop-transfer sequence, we constructed TM1R and TM1-2R, respectively (Figure 4B). Translation of TM1R resulted in a 43-kDa product in the absence of RM (Figure 4C, lane 1). In the presence of RM, a 53-kDa membrane-associated product was also observed (lane 2). PNGase F treatment shifted this 53-kDa band to 43 kDa (lane 3). The change in molecular mass was consistent with four N-linked sugars being added and was further confirmed by limited PNGase F treatment of TM1R products (data not shown). Since four sugar moieties were observed, this suggests that TM1R inserted into membranes in a N_{cyt}-C_{exo} orientation (Figure 4E, model I). This was confirmed by the observation of a 42-kDa product after proteinase K treatment of RM, which shifted to 33 kDa in the presence of endoglycosidase (Figure 4D, lanes 1−3). Therefore, unlike TM7, TM1 contains a strong signal-anchor activity to initiate a N_{cyt}-C_{exo} insertion. Translation of TM1-2R resulted in a 56-kDa product, which shifted to 63 kDa in the presence of RM. This molecular mass change was consistent with three N-linked sugars added and was also confirmed by limited PNGase F treatment (data not shown). A 19-kDa product was observed after proteinase K treatment of RM, and it was shifted to 11 kDa after

endoglycosidase treatment. The 19-kDa peptide represents the glycosylated loop linking TM1 and TM2 (Figure 4E, model II). No protected reporter of 40 kDa was found, suggesting that the reporter in TM1-2R was in the cytoplasmic space. These results strongly suggest that TM2 completely stopped the peptide translocation event.

Translation of TM1/8R resulted in a 56-kDa product in the presence of RM (Figure 4C, lane 8). After treatment with endoglycosidase H (endo H), the 56-kDa product shifted to 48 kDa and was consistent with three N-linked sugars being removed (Figure 4C, lane 9). This was confirmed by visualization of three glycosylated bands after limited endoglycosidase treatment (data not shown). We also treated RM containing TM1/8R with proteinase K and observed a major 19-kDa product that shifted to 11 kDa after endoglycosidase treatment (Figure 4D, lanes 7−9). This 19-kDa product contained three N-linked sugars and likely represents a peptide spanning from TM1 to TM8 (see Figure 4E, model III). These observations are similar to that of TM1-2R. Thus, TM8 also has a stop-transfer activity to stop the membrane translocation event initiated by a signal-anchor sequence (e.g., TM1). Based on these results, we conclude that the alternative topology of Pgp due to the lack of stop-transfer activity of TM8 as shown in Figure 4A less likely exists. Interestingly, we also observed a minor 38-kDa product from the proteinase K digestion of membrane-associated TM1/8R (Figure 4D, lane 7; arrow). It was both endoglycosidase-sensitive (Figure 4D, lane 8; asterisk) and had a mobility that was the same as membrane-protected reporter from both TM7-8R and TM8R. Thus, TM8 also initiates a N_{cyt}-C_{exo} insertion even in the presence of the signal-anchor sequence, TM1 (Figure 4E, model V), confirming its strong signal-anchor activity.

Wheat-Germ Ribosomes Alter the Generation of Two Topological Orientations for the C-Half of Pgp. Recently, we have found that ribosomes are involved in the membrane insertion process for the N-half sequence of Pgp (*23*). To test whether ribosomes also affect the topogenesis of C-half Pgp, we tested the effect of wheat-germ ribosomes on the topological orientation of various Pgp constructs. Translation of the truncated N-half Pgp construct, PGP-N3 (K207V/K210D) (N3R-mut; see ref *25*), resulted in a 57-kDa product (Figure 5, lane 1; see arrow). However, in the presence of wheat-germ ribosomes, a 73% decrease in the 57-kDa product was observed (Figure 5, lane 2). We previously found that this reduction by wheat-germ ribosomes resulted from the inhibition of membrane insertion of TM3 (*23*). When we tested the effect of ribosomes on the C-half TM domain of Pgp (pGHaPGP-C6), we observed a 28% reduction of the glycosylated product in the presence of wheat-germ ribosomes as compared to mammalian ribosomes alone (Figure 5, lanes 3, 4). This suggests that mammalian and wheat-germ ribosomes may also affect the membrane insertion property of C-half Pgp.

To determine the mechanism by which ribosomes affect C-half Pgp membrane topology, we tested the effects of mammalian and wheat-germ ribosomes on the truncated Pgp molecules, TM7-8R, TM8R, and TM1/8R. Compared to mammalian ribosomes, translation in the presence of wheat-germ ribosomes resulted in a pronounced decrease of the generation of the glycosylated product for TM7-8R (80% decrease) and TM8R (53% decrease) (Figure 5, lanes 5−8).

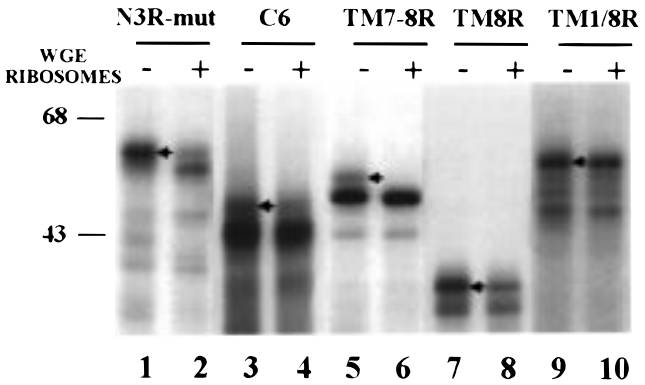

FIGURE 5: Effect of mammalian and wheat-germ ribosomes on generation of C-terminal half Pgp topology. Translation using RRL with RM was performed in the absence or presence of wheat-germ ribosomes for PGP-N3 (K207V/K210D) (N3R-mut), pGHaPGP-C6 (C6), TM7-8R, TM8R, and TM1/8R. Membrane-associated products were obtained and analyzed by SDS−PAGE and densitometry. Arrows denote glycosylated products for each Pgp construct.

However, no change in the glycosylated product was observed for the TM1/8R glycosylated product. Taken together, these results suggest that wheat-germ ribosomes affect the signal-anchor but not the stop-transfer activity of TM8.

DISCUSSION

Several models different from the hydropathy-predicted model have been postulated for the C-half of Pgp. One suggests that TM7 is a signal-anchor sequence and either TM9 or TM10 is a stop-transfer sequence (*14*, *15*, *17*, *18*). This presumably results from the lack of stop-transfer activity for TM8. Another model proposes that TM8 is a signal-anchor sequence that inserts in a N_{cyt}-C_{exo} orientation, while TM7 is comprised of two TM segments (*16*). To resolve this controversy, we examined the mechanism underlying the generation of the various C-half Pgp topologies of Chinese hamster *pgp1* Pgp. Here, we found that the cytoplasmic-predicted loop linking TM8 and TM9 is exposed to the extra-cytoplasmic space because (1) this loop was glycosylated and (2) we were able to immunoprecipitate a peptide after proteinase K treatment using a polyclonal antibody generated against the loop linking TM8 and TM9. This polyclonal antibody was previously found to label the extracellular domain of Pgp in the plasma membrane of MDR cells using immunocytochemistry (*18*). Thus, our results suggest the existence of a topology different from the hydropathy-predicted model for the C-half of the Chinese hamster *pgp1* Pgp. It should be noted that in all of the alternative topologies proposed previously (*14*−*18*), it is common that the loop linking TM8 and TM9 is exposed to the extra-cytoplasmic space.

Our results indicate that TM8 alone can insert into membranes in a N_{cyt}-C_{exo} orientation and thus functions as a signal-anchor sequence. In addition, this function was maintained in the presence of TM7. Thus, our results support the model where TM8 functions as a signal-anchor sequence to insert into membranes in a N_{cyt}-C_{exo} orientation. One implication from these results is that the membrane insertion of TM7 must differ from the hydropathy-predicted model to accommodate the N_{cyt}-C_{exo} insertion of TM8. When we

examined a construct containing TM7 followed by a glycosylation reporter (TM7R), we observed a protein product that was not glycosylated nor associated with membranes. Thus, TM7 lacks de novo membrane insertion activity. This suggests that TM8 rather than TM7 acts as the primary signal-anchor sequence in the C-half Pgp. Recently, Lu et al. (*26*) found that TM2 of the cystic fibrosis transmembrane conductance regulator (or CFTR) has a stronger signal sequence activity than TM1. It was proposed that TM2 of CFTR functions to ensure the proper folding and generation of CFTR transmembrane topology in the event that TM1 fails to insert into membranes. A similar mechanism may exist for the C-half of Pgp where TM8 has stronger signal-anchor activity than TM7. However, we cannot rule out the possibility that a particular sequence of Pgp, which is necessary for the membrane insertion of TM7, was absent from TM7R. For example, TM7 may require an adjacent TM segment in order to insert into membranes. In this regard, we found that translation of TM7-8R resulted in less glycosylated product as compared with TM8R (Figure 3B; compare lanes 2 and 5). One explanation is that TM7 interacts with TM8 such that TM8 insertion in a N_{cyt}-C_{exo} orientation is no longer favored. Interestingly, a cooperative interaction between TM1 and TM2 was previously found to be required for membrane integration of these TM segments to occur (*27*). Assuming that TM7 does fold twice in the membrane, it is also possible that the reinitiation of N_{cyt}-C_{exo} insertion for TM8 in TM7-8R does not readily occur as compared to the de novo insertion of TM8 in TM8R.

It is interesting that the addition of net positive charges C-terminal to putative TM8 resulted in a decrease in glycosylated C-half product, suggesting that lumenal exposure of the loop between TM8 and TM9 is decreased. This result is consistent with the notion that the charge flanking a signal-anchor sequence is a major determinant of the transmembrane orientation for the signal-anchor sequence (*1*). By increasing the net positive charge C-terminal to TM8, a N_{exo}-C_{cyt} orientation would be favored, thus resulting in a cytoplasmic location for the loop linking TM8 and TM9. However, it is important to note that the effect of charge would also be consistent with increasing the potential stop-transfer activity of TM8 and therefore supports the C-half model where TM8 is thought to lack stop-transfer activity while TM7 acts as a signal-anchor sequence. When we examined the stop-transfer activity of TM8, we observed a similar stop-transfer activity for TM8 as compared to TM2. This result suggests that TM8 can also function as a stop-transfer sequence. This finding is consistent with the hydropathy-predicted model where TM7 functions as a signal-anchor sequence to insert into membranes in a N_{cyt}-C_{exo} orientation, and TM8 functions as a stop-transfer sequence.

Recently, we have found that ribosomes may differentially regulate the generation of multiple topological forms of N-terminal half Pgp. When we tested the effect of mammalian and wheat-germ ribosomes on C-half topology, we found that wheat-germ ribosomes decreased the exposure of the loop between TM8 and TM9 to the ER lumen. This effect was likely due to the decreased N_{cyt}-C_{exo} signal-anchor function of TM8 as demonstrated by the decreased glycosylation of TM8R in the presence of wheat-germ ribosomes (Figure 5) and not increased stop-transfer activity of TM8. It is unlikely that wheat-germ ribosomes inhibited glycosylation since wheat-germ ribosomes did not alter the glycosylation of TM1/8R (also see Discussion in ref *23*). These results are consistent with our recent finding that TM3 has decreased signal-anchor activity with wheat-germ ribosomes as compared to mammalian ribosome (*23*). The mechanism by which wheat-germ and mammalian ribosomes differentially regulate the membrane insertion of TM segments is unclear. However, there is growing evidence that ribosomes may be an important factor for the membrane insertion and topology of TM segments. During the translocation process for apolipoprotein B, the ribosome was shown to undergo structural changes, which exposed the nascent chain to the cytoplasmic space (*28*). Recently, Liao et al. found that the TM segment is first recognized by the ribosome, which then triggers structural changes at the translocation machinery (i.e., Sec61p complex) (*29*). Thus, structural changes at the ribosome may be involved in allowing cytosolic proteins and/or the ribosome to facilitate folding, processing, or orientation of the nascent chain.

The ability of TM8 to possess two different types of topogenic information supports the hypothesis that the C-half of Pgp can exist in two topological orientations. When TM8 functions as a stop-transfer sequence, the hydropathy-predicted model will be generated. On the other hand, the signal-anchor activity of TM8 will lead to the generation of a topology different than predicted. This alternate topology may involve the unusual folding properties of putative TM7, which was observed by Béjà and Bibi (*16*). The mechanism by which a cell decides to express either one or both topologies, however, remains an unanswered question.

ACKNOWLEDGMENT

We thank Ms. Crispina Chong-Han for technical assistance and Drs. Steve King, Guillermo Altenberg, and Luis Reuss for their critical reading of an earlier version of the manuscript. We also thank Dr. Mingang Chen, Dr. Ariel Castro, and Ms. Roxana Pinchiera for their helpful discussions and comments on the manuscript.

REFERENCES

1. Spiess, M. (1995) *FEBS Lett. 369*, 76−79.
2. von Heijne, G. (1996) *Prog. Biophys. Mol. Biol. 66*, 113−139.
3. Johnson, A. E. (1997) *Trends Cell Biol. 7*, 90−95.
4. Blobel, G. (1980) *Proc. Natl. Acad. Sci. U.S.A. 77*, 1496−1500.
5. Hartmann, E., Rapoport, T. A., and Lodish, H. F. (1989) *Proc. Natl. Acad. Sci. U.S.A. 86*, 5786−5790.
6. Sipos, L., and von Heijne, G. (1993) *Eur. J. Biochem. 213*, 1333−1340.
7. Gafvelin, G., Sakaguchi, M., Andersson, H., and von Heijne, G. (1997) *J. Biol. Chem. 272*, 6119−6127.
8. Denzer, A. J., Nabholz, C. E., and Speiss, M. (1995) *EMBO J. 14*, 6311−6317.
9. Wahlberg, J. M., and Spiess, M. (1997) *J. Cell Biol. 137*, 555−562.
10. van Klompenburg, W., Nilsson, I., von Heijne, G., and de Kruijff, B. (1997) *EMBO J. 16*, 4261−4266.
11. Gottesman, M. M., and Pastan, I. (1993) *Annu. Rev. Biochem. 62*, 385−427.
12. Loo, T. W., and Clarke, D. M. (1995) *J. Biol. Chem. 270*, 843−848.
13. Kast, C., Canfield, V., Levenson, R., and Gros, P. (1996) *J. Biol. Chem. 271*, 9240−9248.

14. Zhang, J.-T., and Ling, V. (1991) *J. Biol. Chem. 266*, 18224−18232.
15. Skach, W. R., Calayag, M. C., and Lingappa, V. R. (1993) *J. Biol. Chem. 268*, 6903−6908.
16. Béjà, O., and Bibi, E. (1995) *J. Biol. Chem. 270*, 12351−12354.
17. Zhang, J.-T. (1996) *Mol. Biol. Cell 7*, 1709−1721.
18. Zhang, M., Wang, G., Shapiro, A., and Zhang, J.-T. (1996) *Biochemistry 35*, 9728−9736.
19. Pont-Kingdon, G. (1997) *Methods Mol. Biol. 67*, 167−172.
20. Zhang, J.-T., Duthie, M., and Ling, V. (1993) *J. Biol. Chem. 268*, 15101−15110.
21. Zhang, J.-T., and Ling, V. (1993) *Biochim. Biophys. Acta 1153*, 191−202.
22. Walter, P., and Blobel, G. (1983) *Methods Enzymol. 96*, 84−93.
23. Wang, C., Chen, M., Han, E., and Zhang, J.-T. (1997) *Biochemistry 36*, 11437−11443.
24. Fujiki, Y., Hubbard, A. L., Fowler, S., and Lazarow, P. B. (1982) *J. Cell Biol. 93*, 97−102.
25. Zhang, J. T., Lee, C. H., Duthie, M., and Ling, V. (1995) *J. Biol. Chem. 270*, 1742−1746.
26. Lu, Y., Xiong, X., Helm, A., Kimani, K., Bragin, A., and Skach, W. R. (1998) *J. Biol. Chem. 273*, 568−576.
27. Skach, W. R., and Lingappa, V. R. (1993) *J. Biol. Chem. 268*, 23552−23561.
28. Hedge, R. S., and Lingappa, V. R. (1996) *Cell 85*, 217−228.
29. Liao, S., Lin, J., Do, H., and Johnson, A. E. (1997) *Cell 90*, 31−41.

BI980702P